

Study of the population of AGNs with optical jets at milliarcsecond scales

Submitted in response to Research Opportunities in Space and Earth Sciences (ROSES) — 2018 Solicitation, program NNH18ZDA001N-ADAP, Astrophysics Data Analysis.

Contents

1	Introduction	1
2	Predictions and confirmations	3
3	Problem Statement	3
4	Our Approaches and Methodologies	5
4.1	Determination of the spectral energy distribution	5
4.2	Blind search of dependencies of AGN properties on VLBI/ <i>Gaia</i> offsets	8
4.3	Guided search of dependencies of AGN properties on VLBI/ <i>Gaia</i> offsets	9
4.4	Modeling the SED	10
5	Deliverables	10
6	Expected significance of the proposed work	10
7	Management plan	11
7.1	Data sharing plan	11
8	References	12
9	Biographical Sketches	15
10	Summary of Work Effort	17
11	Current and pending support	18
12	Budget Justification: Narration	19
12.1	ADNET Funding	19

1 Introduction

Analysis of VLBI and *Gaia* Data Release 1 (DR1) (Lindgren et al., 2016) position differences of active galactic nuclei (AGNs) has revealed (Petrov & Kovalev, 2017a; Kovalev et al., 2017) that position offsets are not random, but have a preferable direction parallel to the jet direction at parsec scales (see Figure 1. This anisotropy in the distribution of position offsets is highly significant: the probability to have it by chance is below 10^{-11} . At the same time, as it is shown in Figure 2, the VLBI/*Gaia* position offset directions and jet position directions with respect to a direction fixed in the celestial sphere, for instance, the celestial northern pole, do not show any anisotropy.

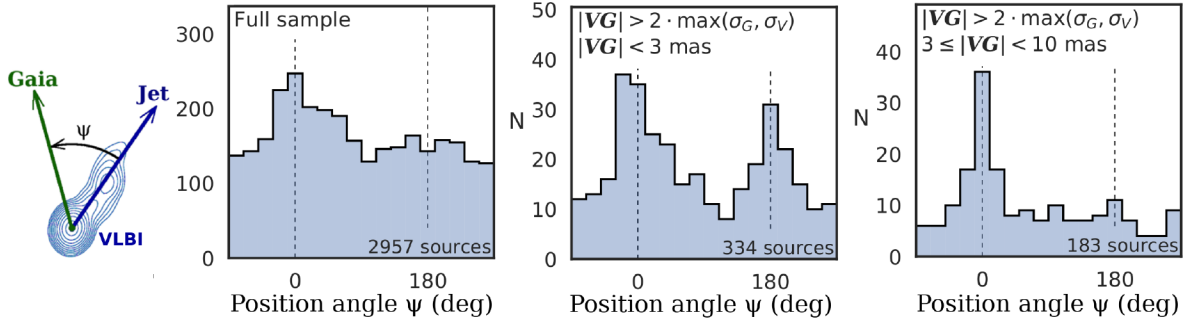


Figure 1: The distribution of VLBI/*Gaia* DR1 position offsets with respect to the jet direction at parsec scales determined with VLBI. *Left*: full sample. *Center*: subsample of the sources with offsets statistically significant at 95% level that are shorter 3 mas. *Center*: subsample of the sources with offsets statistically significant at 95% level that are in a range of 3–10 mas.

The distribution in Figure 1 is produced by subtraction of the quantities which distributions are shown in Figure 2. In the absence of a signal, the difference of two uniformly distributed variable will remain uniformly distributed. This implies that the anisotropy in the distribution is caused by the internal properties of the AGNs, and it is not an artifact of VLBI or *Gaia* techniques.

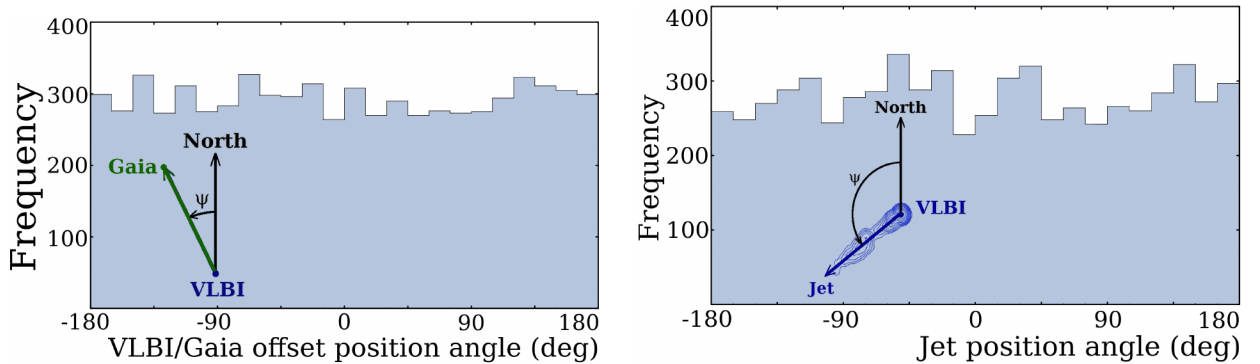


Figure 2: *Left*: the distribution of VLBI/*Gaia* position offsets with respect to the north direction. *Right*: the distribution of AGN jet directions measured with VLBI with respect to the north direction.

The suggested explanation is the presence of optic jets at scales 1–100 mas, i.e. within the point spread function (PSF) of *Gaia*, since as a detailed analysis given in Petrov & Kovalev

(2017b) has shown, other possible *systematic* effects, namely the core-shift and the contribution of source structure on VLBI positions, are more than one order of magnitude too small to explain the phenomenon. The presence of observed VLBI/*Gaia* offsets does not automatically mean that optical and radio emission is generated in different regions. Even in the case if radio and optical emission is co-spatial, i.e. location of the core and the jet in radio and optical ranges coincide, position estimates from VLBI and *Gaia* may be different because a response on an extended source of a power detector used by *Gaia* and an interferometer that records voltages is fundamentally different. When the source structure is confined within the PSF, the position determined by a power detector corresponds to the position of an image centroid, while position determined by an interferometer is very close to the position of the most compact image component.

Therefore, VLBI/*Gaia* position difference is an offset of an optical image centroid with respect to the position of a radio core associated with the jet origin.

Optical and X-ray jets at AGNs are not uncommon. They are known at about 20 sources and studied in detail in (refs). Known optical jets at scales 0.2–20 arcsec are co-spatial with radio jets. In order to explain histogram 1, we suggest that known optical jets are the tail of the distribution, and at scales 1–200 mas the optical jets are ubiquitous. Figure 3 presents the simplified diagram. The green ellipse shows the position of the radio core — the area of the optically thick jet. The radio core is assumed to be displaced with respect to the accretion disk toward jet direction. In general, the radio core is displaced with respect to the optical core along the jet, but multifrequency VLBI observations allows to evaluate the magnitude of this shift (refs) and relate position of the radio core to position of the the optical core. The optically thin jet is shown with blue color. The optical position measured by *Gaia* denoted by a cross, is the centroid of the three-component image: accretion disk, core, and the jet. It depends on fluxes and relative distances of the components. We introduce two fundamental observables \mathcal{O}_j and \mathcal{O}_t — projection of the *Gaia* position offset with respect to the VLBI position into the parsec-scale jet direction determined from a VLBI image.

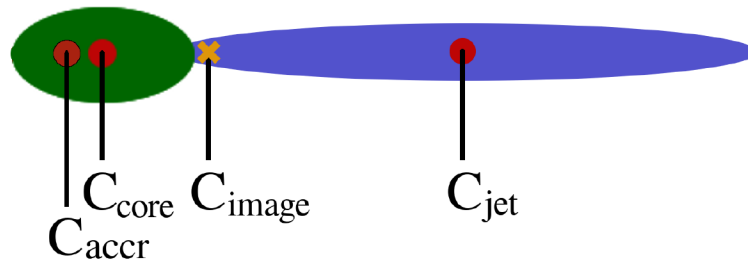


Figure 3: The diagram of the core-jet morphology. Red circles are centroids of the accretion disk, core, and optically thin jet. The image centroid is the centroid of these three components.

If emission of the optical jet is negligible, the image centroid will be close to the accretions disk, and \mathcal{O}_j will be negative. Strong emission from the optical jet can shift the image centroid along the jet and make \mathcal{O}_j positive. Thus, \mathcal{O}_j is a measure of optical jet dominance. This is a new source of information, not known before *Gaia* data release, and the focus of our project is to use it for the AGN population study.

2 Predictions and confirmations

The presence of optical structure results in a number of observational consequences. One of them is a prediction of a jitter in optical positions of radio-loud AGNs due to variability (Petrov & Kovalev, 2017b). Analysis of light curves and position jitter from *Gaia* with respect to VLBI positions will allow us to measure *quantitatively* the distance of the jet centroid with respect to the jet base, distance between the jet base and the accretion disk, and the share of jet flux in optical range to the total flux for the sources with strong variability or flaring events during *Gaia* mission. We will be able to check these prediction in 2022 after *Gaia* DR4. We made another prediction: the anisotropy in VLBI/*Gaia* jet directions will not disappear with the grow of accuracy, but offsets will be determined just more precisely. In particular, we predicted the peaks in the histogram will become sharper. Figure 4 demonstrates the same histogram, but generated using *Gaia* DR2 (Lindgren et al., 2018) that was made publicly available on April 25, 2018. The anisotropy indeed became more profound than in *Gaia* DR1 due to higher position accuracy of DR2!

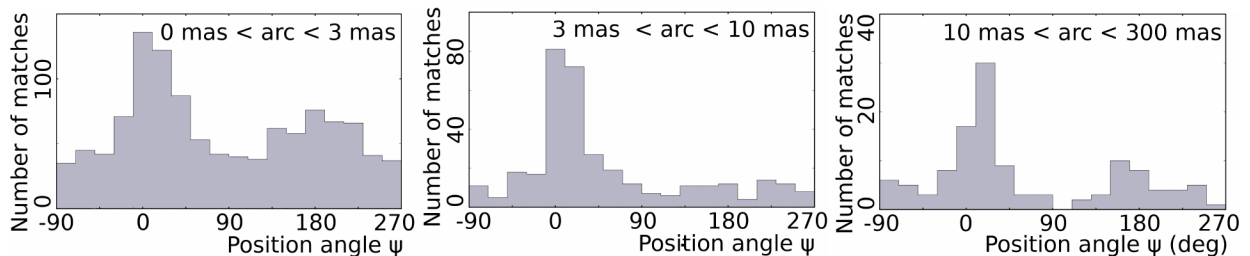


Figure 4: The distribution of statistically significant VLBI/*Gaia* position offsets using *Gaia* DR2. The peaks of the distributions are sharper than the same histogram generated using *Gaia* DR1, because position errors of *Gaia* DR2 are significantly lower.

Our interpretation of VLBI/*Gaia* offsets as manifestation of the presence of optical disk results in a separation of sources that are tentatively accretion disk dominated and jet dominated. Jet dominant in this contest does not necessarily means jet contribution is greater than accretion disk contribution. Since thermal emission of the accretion disk and synchrotron emission of the jet have different spectrum, we predicted the sub-sample with position angles around 0 (jet-dominant) and position angles around 180° (accretion disk dominant) will have a different color. A cursory look at the *Gaia* DR2 data that were released one week before this project is prepared has confirmed that the colors of two sub-samples are indeed different. As we see in Figure 5 that the sources with optical centroid shifted along the jet with respect to the jet base are systematically redder.

Predictions that are confirmed provide a very strong argument that our interpretation is valid. Diagrams like Figure 5 present a strong evidence that investigation of statistical dependencies of \mathcal{O}_j observables and offset position angles will allow us to study properties of optical jets at 0.1–100 mas scales.

3 Problem Statement

Cross-matching VLBI and *Gaia* DR2 catalogues of AGN positions, we cross-matched 8801. We determined jet directions of 4027 matches and computed \mathcal{O}_j and \mathcal{O}_t observables. Of them,

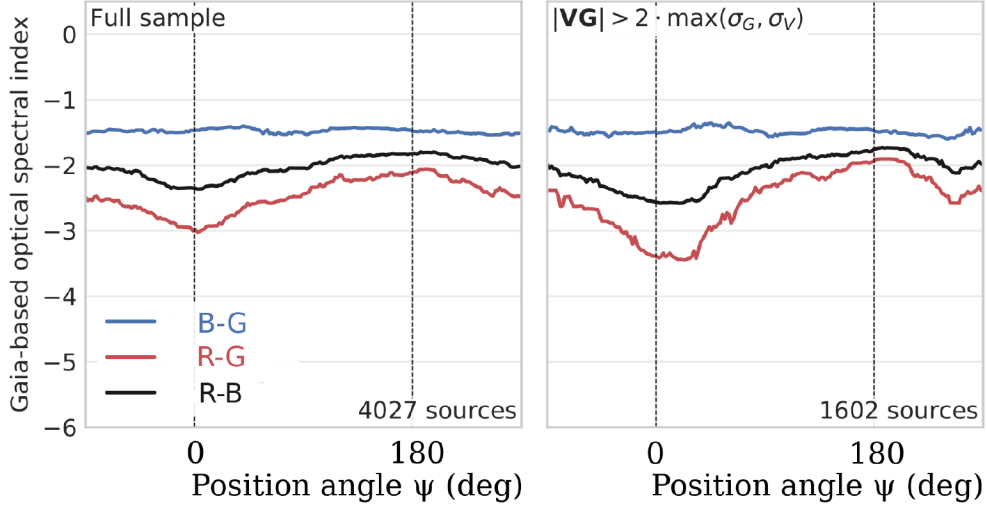


Figure 5: The histogram of spectral indices ($S \sim f^{+\alpha}$) of VLBI/*Gaia* matches derived using G, B, and R fluxes provided by *Gaia* DR2. Angle ψ is the direction of *Gaia* position offset relative to VLBI position with respect to jet direction. *Left*: full sample. *Right*: sub-sample of statistically significant offsets. The histogram was smoothed with the moving median with $\pm 50^\circ$ window.

1649 sources have offsets greater $2 \max(\sigma_G, \sigma_V)$, i.e. statistically significant. We split the sample of 4027 AGNs into three sub-samples: P_s with $\sigma(\mathcal{O}_j) > 2 \max(\sigma_G, \sigma_V)$ (734 sources), N_s with $\sigma(\mathcal{O}_j) < -2 \max(\sigma_G, \sigma_V)$ (383 sources), and 2910 others. According to the argumentation presented in the previous section, we consider the sources of the first sub-sample P_s as having significant contribution from both optically thick and optically thin jet in the optical range. We consider that the sources from the second sub-sample N_s have a low contribution from jets. We split the remaining sources into two sub-samples: P_n if $\mathcal{O}_j > 0$ (1529 sources) and N_n if $\mathcal{O}_j \leq 0$ (1381 sources). The last two sub-samples discriminate the populations of sources with significant and insignificant jet contribution, but \mathcal{O}_j is not significant for a given source.

The objective of our project is to investigate the differences in statistics of AGN properties in samples P_s against N_s and P_n against N_n , i.e. investigate to what extent the presence of the significant contribution of optical emission from the jet affects properties of radio-loud AGN.

The motivation of our study is to find the use of a new information about AGN properties, \mathcal{O}_j and \mathcal{O}_t observables, that was not available before September 2016 and try to exploit it to better understanding the AGN nature. It was assumed that optical emission from AGNs has a thermal component from the accretion disk and a non-thermal component from the jet. However, in the past there were no method to measure the contribution of the non-thermal emission. The basic question that we are going to investigate is how the presence of a strong optical jet affects other properties of AGNs. Are the radio-loud AGNs with strong optical jet dominance are different than the AGNs with weak jets? Studying sub-samples with > 1000 objects is promising to provide robust statistics.

4 Our Approaches and Methodologies

There are 8801 matches of VLBI and *Gaia* with the probability of false association < 0.0002 . Among them, jet directions have been determined for 4027 objects, i.e. roughly for one half. The VLBI/*Gaia* position offsets with respect to jet direction was published by Petrov & Kovalev (2017a). We have determined \mathcal{O}_j and \mathcal{O}_t observables for these sources based on that publication and corrected by subtracting *Gaia* DR2 minus *Gaia* DR1 difference, transforming VLBI/*Gaia* DR1 offsets in the original publication to VLBI/*Gaia* DR2 offsets. These objects form the parent sample that we are going to investigate in detail.

Our approach consists of three tasks:

1. Determine spectral energy distribution (SED) in the sample of 8801 matches using all ranges from radio to γ -ray. We will use both space-born and ground catalogues. For this task we do not restrict ourselves with the parent sample and consider all 8801 matches, anticipating that the number of sources with known jet directions will grow within next several years owing to new VLBI programs that are currently running.
2. Investigate correlations between \mathcal{O}_j , and \mathcal{O}_t observables or the position angle with respect to fluxes, spectral indices and other derived parameters.
3. To model the SED in order to separate the contribution from starlight, accretion disk, and the jet. To model the distribution of \mathcal{O}_j and \mathcal{O}_t observables and investigate, whether there is a contradiction between these two models.

4.1 Determination of the spectral energy distribution

We will use the following datasets to determine flux of the matched objects:

- **GALEX** We will be using Revised GALEX catalog (Bianchi et al., 2017). This catalogue will provide us the magnitudes of matched objects at 152.8 nm (Far UV) and 231 nm (near UV). A preliminary analysis identified 51% VLBI/*Gaia* matches have a counterpart in GALEX catalogue. Median arc length, $0.83''$, makes final association relatively simple. We will need to assess the source density at the grid of galactic longitude and latitude, and using the source density to compute the probability to find an unrelated object within a given search radius, similar to what we have done in (Petrov & Kovalev, 2017a). We are going to scrutinize each source paying special attention to extended sources.
- **ROSAT** We will be using ROSAT all-sky survey bright source catalogue (Voges et al., 1999) and The ROSAT All-Sky Survey Faint Source Catalogue (RASS-FSC) (Voges et al., 2000) for getting source fluxes at 0.1–2.4 keV and two hardness ratios that are proportional to spectral indices in the soft (0.1–0.4 keV) and hard (0.5–2.0 keV) energy bands. A preliminary analysis identified 30% matches have a ROSAT counterpart within $180''$. This cutoff seems a bit excessive and a simple association using this cutoff may have 1–2% fraction of false association. We will investigate the optimal arc length cutoff using $\log N$ – $\log S$ for VLBI/X-ray association, evaluate source density as a function of galactic latitude and the probability of false association at a given arc length, source flux and warning flags.

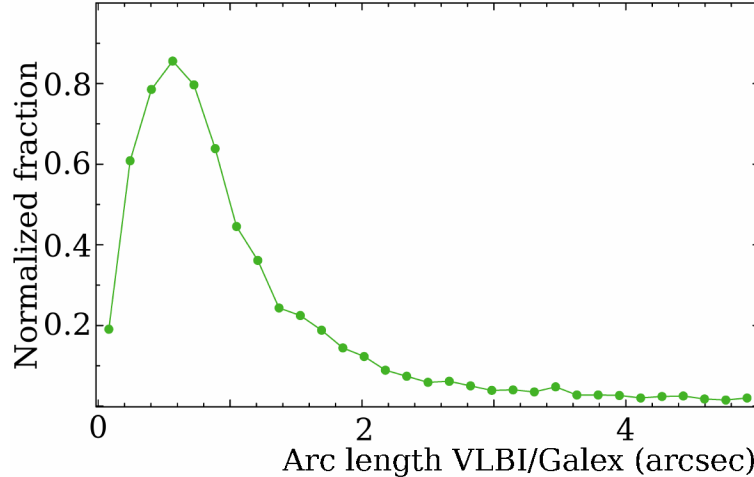


Figure 6: Distribution of arc-lengths between GALEX and VLBI positions. The distribution is normalized to have integral equal to 1.

- 2CXO** A fraction of sources detected with ROSAT was observed with Chandra. We will be using 2CXO catalogue available at <http://cxc.harvard.edu/csc2/> that is an extension of 1CXO catalogue (Evans et al., 2010). Position accuracy of Chandra is relatively high, the median arc length between VLBI and 2CXO is 0.2 mas, which makes association with 2CXSO relatively easy. Approximately 5% of VLBI/*Gaia* matches have a Chandra counterpart. We will use fluxes from broad (0.5–7.0 keV) and hard bands (2.0–7.0 keV).
- WISE** We will be using ALL-WISE catalogue (Wright et al., 2010) to get far-infrared fluxes at 3.4, 4.6, 12, and 22 μm . A preliminary analyze identified 87% VLBI/*Gaia* matches have a counterpart in WISE catalogue. We are going to scrutinize each source paying special attention to extended sources and crowded zones.
- Fermi** We will be using the Preliminary LAT 8-year catalogue available at <https://fermi.gsfc.nasa.gov/ssc/data/access/lat/fl8y> that is an extension of the LAT 4-year Catalog 3FGL (Acero et al., 2015) to get the energy flux at the band 100–1000 MeV and 1–100 GeV. We have developed our own efficient method for association of *Fermi* sources with VLBI (Petrov et al., 2013; Schinzel et al., 2015, 2017) based on computation of the the ratio of the probability that a radio counterpart of *Fermi* source will be found inside a disk of a given search radius to the probability to find a background radio source with a given flux density or greater *outside* the same disk. A preliminary analyze showed that 23% VLBI/*Gaia* matches have a counterpart in *Fermi* catalogue.
- PanSTARRS** We will be using PanSTARRS catalogue (Chambers et al., 2016) to get near-infrared fluxes at i, z, and y bands. A preliminary analyze identified 87% VLBI/*Gaia* matches have a counterpart in PanSTARRS catalogue within its sky coverage. We will perform similar matching analysis as for GALEX and WISE.
- SkyMapper** We will be using SkyMapper catalogue (Wolf et al., 2018) to get fluxes at u, v, i, and z, bands of the southern hemisphere sources brighter 18 mag at g filter. A preliminary

Table 1: Table of frequency ranges for SED computation. Flag: whether a given instrument is one of space astrophysics missions with NASA significant contribution.

Range	Instrument	Flag	Status
2.2–2.4 GHz	VLBI	No	finished
8–9 GHz	VLBI	No	finished
22 μm	WISE	Yes	Proposed
12 μm	WISE	Yes	Proposed
4.6 μm	WISE	Yes	Proposed
3.4 μm	WISE	Yes	Proposed
Y-filter	PanSTTARS	No	Proposed
Z-filter	PanSTTARS, SkyMapper	No	Proposed
I-Filter	PanSTTARS, SkyMapper	No	Proposed
R-Filter	Gaia DR2	No	finished
G-Filter	Gaia DR2	No	finished
B-Filter	Gaia DR2	No	finished
U-Filter	SkyMapper	No	finished
231 nm	GALEX	Yes	Proposed
153 nm	GALEX	Yes	Proposed
0.1–0.4 kv	ROSAT	Yes	Proposed
0.5–2.0 kv	ROSAT	Yes	Proposed
2.0–7.0 keV	Chandra	Yes	Proposed
0.1–1 GeV	Fermi	Yes	Proposed
1–100 GeV	Fermi	Yes	Proposed

analyze identified 10% VLBI/*Gaia* matches have a counterpart in PanSTARRS catalogue within its sky coverage. We will perform similar matching analysis as for GALEX and WISE.

Table 4.1 summarizes the frequency (energy) ranges for SED computation. We should emphasize that although the use of *Gaia* and VLBI data is essential for our project, we do not propose work related with VLBI and *Gaia*. VLBI data analysis that includes precise astrometry and imaging is finished and published. Association with *Gaia* is finished and published. Fluxes at B, G, and R filters have been extracted during VLBI-*Gaia* association and do not require extra work. The focus of this task is to associate VLBI objects with space-born detectors and build reliable SED. Exploratory nature of our project dictates selection of broad range of observables that can be used to reveal the dichotomy between jet-dominated and accretion disk dominated radio-loud AGNs.

We will collect redshifts for the parent samples first using NASA/IPAC Extragalactic Database (NED) and then performing a thorough literature search for the redshifts that are not yet in the NED. Currently, approximately 40% objects from the VLBI have known redshifts.

We will establish AGN classification, such as quasar, BL Lac, galaxy, using Extragalactic Database (NED) and then performing a thorough literature search using SDSS and other sources

of information. We are going to estimate source compactness in UV (GALEX), IR (WISE) and optic (PanSTARRS) by processing images and integrating fluxes within several circles of fixed radius. These estimates will allow us to assess the contribution of starlight.

We are going to scrutinize GALEX, WISE, PanSTARRS, and SkyMapper images and flag interacting galaxies.

4.2 Blind search of dependencies of AGN properties on VLBI/*Gaia* offsets

Since a study of VLBI/*Gaia* position offsets is a new research area that did not exist even two years ago, the first phase is exploratory. We will consider two primary observables, \mathcal{O}_j and \mathcal{O}_t , and the derived quantity, position angle ψ and will perform a blind search of dependencies similar that we showed in Figure 5. Another very preliminary result of such blind search is shown in Figure 7: the sources with position angle ψ around 180° that we tentatively consider as accretion disk dominated (weak jet) are predominately brighter.

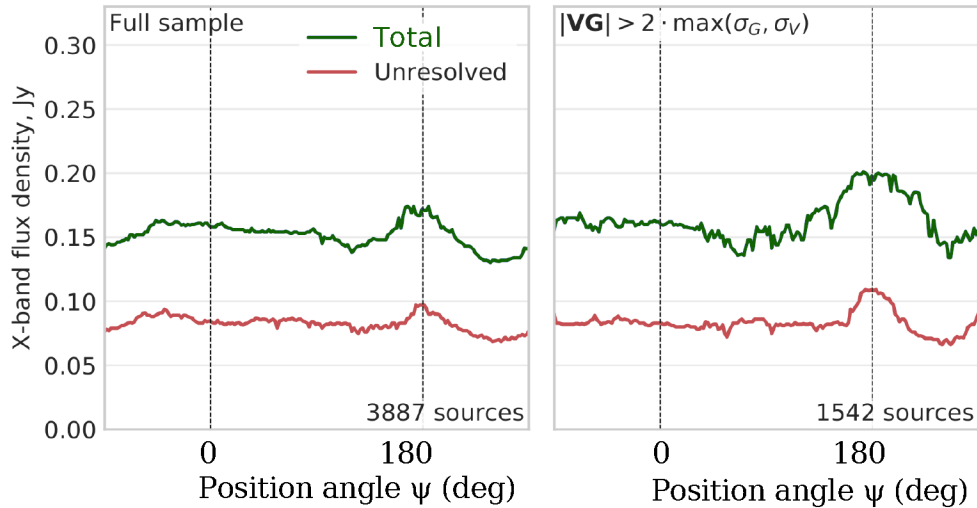


Figure 7: The histogram of the dependencies of flux density at 8 GHz of VLBI/*Gaia* matches as a function of the *Gaia* position offset ψ with respect to jet direction. The total flux density is integrated over the image and is confined to 10 mas area. The unresolved flux density characterizes the radio flux density at sub-mas scales. *Left*: full sample. *Right*: sub-sample of statistically significant offsets. The histogram was smoothed with the moving median with $\pm 50^\circ$ window.

These two results are low-hanging fruits, since *Gaia* colors were taken directly from *Gaia* and flux densities from the VLBI database available at http://astrogeo.org/vlbi_images that we have developed in the past. Collection of information about multi-frequency broad-band fluxes and computation of the SED from radio to hard γ -ray range will significantly expand the parameters space and enables us to perform a search of such dependencies in a systematic way.

In particular, we are going to perform a blind search and explore the following relationships:

- histograms of dependence of fluxes at different ranges similar to those presented in Figure 7;

- histograms of dependence of colors at different ranges similar to those presented in Figure 5;
- relationships between \mathcal{O}_j and \mathcal{O}_t observables or position angles ψ against fluxes and colors.
- relationships between \mathcal{O}_j and \mathcal{O}_t observables or position angles ψ against source compactness in optic and radio,
- relationships between \mathcal{O}_j and \mathcal{O}_t observables or position angles ψ against distance derived from redshifts.

The dataset used in the blind search will be subdivided by the source classes and other characteristics, such as the presence of interacting galaxy.

Blind search is aiming to find basic relationships, including those that are not expected. Results of blind search will augment the list of relationships for guided search.

4.3 Guided search of dependencies of AGN properties on VLBI/*Gaia* offsets

In addition to blind search, we are going to perform a guided search based on our expectation of what kind of dependencies we can find. We expect that sources with negative \mathcal{O}_j observables have less powerful optic jets than those with large positive \mathcal{O}_j and they have large share of thermal emission from the accretion disk. This SED that includes IR, optical, UV, and soft X-ray emission is supposed to help to identify the contribution of the Big Blue Bump — a significant feature in the UV to optical region. This feature is thought to be thermal emission from an optically thick accretion disk feeding a massive black hole. This was one of the motivations of using GALEX and ROSAT data for our study. We are also going to estimate the IR bump with maximum at 2–10 μm that is generally attributed to thermal emission from dust at temperatures of order 100–1000 K. We will parameterize the strength of the Big Blue Bump and the strength of the IR bump in the SED with a simple mathematical model of a broken power-law requiring that emission features at wavelengths below a given cutoff to corresponds the specified region.

We will investigate the relationships of these parameters of with \mathcal{O}_j and position angle ψ . We expect the strength of the Big Blue Bump will correspond to the relative strength of the accretion disk emission and we expect the source with large Big Blue Bump will be more common in the population with negative \mathcal{O}_j . Strength of the IR bump is expected to correlate with the abundance of dist and dust obscuration. We will check whether the sources with strong IR bumps will are less common in the population objects with negative \mathcal{O}_j . We will also perform in depth guided search for the relationships established during the coarse search.

An important part of guided search procedure is evaluation of a selection bias. As the $\log N - \log S$ curves suggests the parent VLBI catalogue is completed to a level of 150 mJy, but it contains also sources as weak as 10 mJy. *Gaia* is complete at around 21 mag at G filter, and thus cuts approximately 40% VLBI sources that are weaker. The GALEX All-Sky Imaging Survey is complete at about 21 mag at 231 nm and 20 mag at 153 nm. Basically, for each characteristics, flux density at a given wavelength, redshift, source class, we have a different subset of sources that. Neither subset is complete. We will investigate the impact of the selection basis at a case by case basis by examining the procedure how the subset was formed and by drawing sub-samples that are complete at certain criteria

4.4 Modeling the SED

We are going to model the SED in our sample in order to separate start-burst and accretion disk emission. As a starting point, we are going to use the Markov Chain Monte Carlo based AGNfitter (Rivera et al., 2016). We will consider four independently modeled component, specifically, the accretion disk emission the hot dust surrounding the accretion disk (torus), and the stellar population of the host galaxy, and the emission from the cold dust in star-forming regions. The parameter space has ten adjustable parameters. The most important parameters for our study the integrated accretion disk luminosity and the integrated host galaxy emission in the frequency range of the G filter.

We are going to explore whether the objects with large \mathcal{O}_t observables, i.e. with VLBI/*Gaia* position offsets that are misaligned with respect to the jet direction are predominantly in the objects with significant fraction of host galaxy emission. In general, the AGNs may be misaligned with respect to the center of host galaxy optical emission at several milliarcsecond level. The contribution of such a misalignment to the centroid offset will be for the AGNs with a large share of host galaxy emission.

We expect the sources with large negative \mathcal{O}_j observables will have larger fraction emission from the accretion disk from the SED model. We are going to check whether the SED modeling will confirm this.

We will explore whether the SED fitting algorithm can be extended as include the contribution of the synchrotron jet emission without introducing degeneracies.

5 Deliverables

The following will be delivered in the course of the project:

- Associations of VLBI/*Gaia* matches with WISE, PanSTARRS, SkyMapper, GALEX, ROSAT, Chandra, *Fermi* catalogues.
- Broad band spectrum of VLBI/*Gaia* matches compiled from associations with above mentioned catalogues
- AGN classification and known redshifts of VLBI/*Gaia* matches associations with above mentioned catalogues
- The results of modeling the SED of VLBI/*Gaia* matches
- significant relationships between \mathcal{O}_j \mathcal{O}_t observables, and the position angle ψ against parameters of the broad-band photometry, colors, and parameters of the SED model.

6 Expected significance of the proposed work

We are going to fully explore the potential that measurement of the offset in an optical image centroid with respect to the position of a radio core associated with the jet origin brings to understanding the population of radio-loud AGNs.

The goal of our project is to bring new observables, \mathcal{O}_j and \mathcal{O}_t into the mainstream of AGN astrophysics.

7 Management plan

The chart below shows the schedule for implementing the tasks. The schedule is arranged to give an approximately uniform deployment of effort for the team.

Table 2: Schedule chart

Activity name	PY1 H1	PY1 H2	PY2 H1	PY2 H2
Association of VLBI/ <i>Gaia</i> matches	•	•		
Compiling the broad-band AGNs spectra	•	•		
Investigation of relationships within the sample	•	•	•	
SED modeling		•	•	•
Writing papers and reports				•

The Principal Investigator, Leonid Petrov, who works for ADNET Systems Inc. will manage the project. He will be compiling the broad-band AGNs spectra, investigate the relationship within the sample and work on SED modeling.

Alexander Plavin, who is the 2nd year PhD student of the Astro Space Center of Lebedev Physical Institute will be working on SED modeling, investigation of empirical relationships within the sample and investigation of impact of sample incompleteness.

Professor Yuri Kovalev will work on interpretation of results. He will manage work of Alexander Plavin.

7.1 Data sharing plan

The major results of this project will be accessible as electronic attachments to peer-reviewed publications. In addition, to provide a wide visibility of results to the community, we will maintain the project web site that will contain these results as well as auxiliary data products ... Examples of our past data-sharing practices can be found at <http://astrogeo.org>

8 References

- Acerro, F., Ackermann, M., et al.(2015). “Fermi Large Area Telescope Third Source Catalog”, *Astrophys. J. Supp.*, 218, 23A
- Bianchi, L., Shiao, B., Thilker, D., (2017). “Revised Catalog of GALEX Ultraviolet Sources. I. The All-sky Survey: GUVcat_AIS”, *Astrophys. J. Supp.*, 230, 24B.
- Chambers, K. C.; Magnier, E., et al., (2016), “The Pan-STARRS1 Surveys”, [arxiv.org:1612.05560](https://arxiv.org/abs/1612.05560).
- Evans, I. N., Primini, F. A., Glotfelty, K. J., Anderson, C. S., Bonaventura, N. R., Chen, J. C., Davis, J. E., Doe, S. M., Evans, J. D., Fabbiano, G. Galle, Elizabeth C., Gibbs, D. G., Grier, J. D., Hain, R. M., Hall, D. M., Harbo, P. N., He, X. Helen, Houck, J. C., Karovska, M. Kashyap, Vinay, L., Lauer, J., McCollough, M. L., McDowell, J. C., Miller, J. B., Mitschang, A. W., Morgan, D. L., Mossman, A. E., Nichols, J. S., Nowak, M. A., Plummer, D. A., Refsdal, B. L., Rots, A. H., Siemiginowska, A. Sundheim, Beth, A., Tippetts, M. S., Van Stone, D. W., Winkelman, S. L., Zografou, P., (2010), “The Chandra Source Catalog”, *Astrophys. J. Supp.*, 189, 37E.
- Kovalev, Y.Y., Petrov, L., Plavin, A. V, (2017). “VLBI-Gaia offsets favour parsec-scale jet direction in Active Galactic Nuclei”, *Astron. & Astrophys.*, 598, L1.
- Lindgren, L., Lammers, U., Bastian, U., Hernandez, J., Klioner, S., Hobbs, D., Bombrun, A., Michalik, D., Ramos-Lerate, M., Butkevich, A., Comoretto, G., Joliet, E., Holl, B., Hutton, A., Parsons, P., Steidelmüller, H., Abbas, U., Altmann, M., Andrei, A., Anton, S., Bach, N., Barache, C., Becciani, U., Berthier, J., Bianchi, L., Biermann, M., Bouquillon, S., Bourda, G., Brüsemeister, T., Bucciarelli, B., Busonero, D., Carlucci, T., Castaneda, J., Charlot, P., Clotet, M., Crosta, M., Davidson, M., de Felice, F., Drimmel, R., Fabricius, C., Fienga, A., Figueras, F., Fraile, E., Gai, M., Garralda, N., Geyer, R., Gonzalez-Vidal, J. J., Guerra, R., Hambly, N. C., Hauser, M., Jordan, S., Lattanzi, M. G., Lenhardt, H., Liao, S., Lüffler, W., McMillan, P. J., Mignard, F., Mora, A., Morbidelli, R., Portell, J., Riva, A., Sarasso, M., Serraller, I., Siddiqui, H., Smart, R., Spagna, A., Stampa, U., Steele, I., Taris, F., Torra, J., van Reeve, W., Vecchiato, A., Zschocke, S., de Bruijne, J., Gracia, G., Raison, F., Lister, T., Marchant, J., Messineo, R., Soffel, M., Osorio, J., de Torres, A., O’Mullane, W., (2016). “Gaia Data Release 2: The astrometric solution Gaia Data Release 1. Astrometry: one billion positions, two million proper motions and parallaxes”, *Astron. & Astrophys.*, 594, 4L.
- Lindgren, L., Hernandez, J., Bombrun, A., Klioner, S., Bastian, U., Ramos-Lerate, M., de Torres, A., Steidelmüller, H., Stephenson, C., Hobbs, D., Lammers, U., Biermann, M., Geyer, R., Hilger, T., Michalik, D., Stampa, U., McMillan, P. J., Castaneda, J., Clotet, M., Comoretto, G., Davidson, M., Fabricius, C., Gracia, G., Hambly, N. C., Hutton, A., Mora, A., Portell, J., van Leeuwen, F., Abbas, U., Abreu, A., Altmann, M., Andrei, A., Anglada, E., Balaguer-Nunez, L., Barache, C., Becciani, U., Bertone, S., Bianchi, L., Bouquillon, S., Bourda, G., Brusemeister, T., Bucciarelli, B., Busonero, D., Buzzi, R., Cancelliere, R., Carlucci, T., Charlot, P., Cheek, N., Crosta, M., Crowley, C., de Bruijne, J., de Felice, F., Drimmel, R., Esquej, P.,

- Fienga, A., Fraile, E., Gai, M., Garralda, N., Gonzalez-Vidal, J. J., Guerra, R., Hauser, M., Hofmann, W., Holl, B., Jordan, S., Lattanzi, M. G., Lenhardt, H., Liao, S., Licata, E., Lister, T., Löffler, W., Marchant, J., Martin-Fleitas, J.-M., Messineo, R., Mignard, F., Morbidelli, R., Poggio, E., Riva, A., Rowell, N., Salguero, E., Sarasso, M., Sciacca, E., Siddiqui, H., Smart, R. L., Spagna, A., Steele, I., Taris, F., Torra, J., van Elteren, A., van Reeve, W., Vecchiato, A., (2018), “Gaia Data Release 2: The astrometric solution”, [arxiv.org/1804.09366](https://arxiv.org/abs/1804.09366)
- Petrov, L., Kovalev, Y.Y., (2017a). “On significance of VLBI/Gaia offsets”, *Mon. Not. Roy. Astr. Soc. Let.*, 467, L71–L75.
- Petrov, L., Kovalev, Y.Y., (2017b). “Observational consequences of optical range milliarcsecond-scale structure in active galactic nuclei discovered by Gaia”, *Mon. Not. Roy. Astr. Soc.*, 471, 3775–3787.
- Petrov, L., Mahony, E. K., Edwards P. G., Sadler E. M., Schinzel, F. K., (2013). “ATCA observations of Fermi unassociated sources”, *Mon. Not. Roy. Astr. Soc.*, 432, 1294–1302.
- Rivera, G., Lusso, E., Hennawi, J.H., and Hogg, D.H., (2016). “AGNfitter: a bayesian MCMC approach to fitting spectral energy distributions of AGNs”, *Astrophys. J.*, 833:98 (20pp).
- Schinzel, F.K., Petrov, L., Taylor, G.B., Edwards, P.G. 2017. “Radio Follow-up on all Unassociated Gamma-ray Sources from the Third Fermi Large Area Telescope Source Catalog”, *Astrophys. J.*, 838, 139S.
- Schinzel, F. K., L. Petrov, G. Taylor, E. Mahony, P. Edwards, Y. Kovalev, 2015. “New Associations of Gamma-Ray Sources from the Fermi Second Source Catalog”, *Astrophys. J. Supp.*, 217, 4S.
- Voges W., B. Aschenbach, Th. Boller, H. Bräuninger, U. Briel, W. Burkert, K. Dennerl, J. Engenhauser, R. Gruber, F. Haberl, G. Hartner, G. Hasinger, M. Kürster, E. Pfeffermann, W. Pietsch, P. Predehl, C. Rosso, J.H.M.M. Schmitt, J. Trümper, and H.-U. Zimmermann, (1999). The ROSAT All-Sky Survey Bright Source Catalogue (1RXS), *Astron. & Astrophys.*, 349, 389–405.
- Voges W., Aschenbach B., Boller Th., Brauninger H., Briel U., Burkert W., Dennerl K., Engenhauser J., Gruber R., Haberl F., Hartner G., Hasinger G., Pfeffermann E., Pietsch W., Predehl P., Schmitt J., Trumper J., Zimmermann U., (2000). “ROSAT All-Sky Survey Faint source Catalogue (RASS-FSC)” *IAU Circ.* 7432.
<http://www.xray.mpe.mpg.de/rosat/survey/rass-fsc>
- Wolf, C., Onken, C. A., Luvaul, L. C., Schmidt, B. P., Bessell, M. S., Chang, S.-W., Da Costa, G. S., Mackey, D., Martin-Jones, T., Murphy, S. J., Preston, T., Scalzo, R. A., Shao, L., Smillie, J., Tisserand, P., White, M. C., Yuan, F., “SkyMapper Southern Survey: First Data Release (DR1)”, *Publ. Astron. Soc. Australia*, 35, e010.
- Wright, E. L., Eisenhardt, P. R. M., Mainzer, A. K., Ressler, M. E., Cutri, R. M., Jarrett, T., Kirkpatrick, J. D., Padgett, D., McMillan, R. S., Skrutskie, M., Stanford, S. A.; Cohen, M. Walker,

Russell G., Mather, J. C., Leisawitz, D., Gautier, T. N.; McLean, I., Benford, D., Lonsdale, C. J., Blain, A., Mendez, B., Irace, W. R., Duval, V., Liu, F., Royer, D., Heinrichsen, I., Howard, J., Shannon, M., Kendall, M., Walsh, A. L., Larsen, M., Cardon, J. G., Schick, S.; Schwalm, M., Abid, M., Fabinsky, B., Naes, L., Tsai, C.-W., (2010), “The Wide-field Infrared Survey Explorer (WISE): Mission Description and Initial On-orbit Performance”, *Astron J*, 140, 1868W.

9 Biographical Sketches

Leonid Petrov (PI)

Present position:

Principal Scientist of ADNET Systems Inc.

Professional experience:

Since 1988 Leonid Petrov has been working in data analysis of VLBI data for various applications. He has developed algorithms and implemented them into software for all phases of VLBI technique that includes scheduling, VLBI post-correlation processing based on cross-spectrum, computation of theoretical VLBI delay, astrometric VLBI data analysis based on group delays, and imaging. He has processed all publicly available VLBI observations suitable for astrometry and geodesy (over 140,000 hours) and reprocessed from visibility level (Level 1B) all VLBA astrometric observing campaigns. Leonid Petrov participated as a PI or co-I of the majority of VLBI astrometry program. He has compiled the most comprehensive astrometric catalogue of VLBI sources, publicly available at <http://astrogeo.org/rfc>, that by May 2018 has 14,786 entries. Position accuracy of that catalogue is close to the position accuracy of *Gaia*. He has produced over 25,000 VLBI images, and he maintains the most complete database of VLBI source images, publicly available at http://astrogeo.org/vlbi_images of over 12,000 extragalactic sources.

His work as NASA contractor involved improvement of VLBI technique, designing and running global VLBI astrometry program, implementation of advanced methods of VLBI data analysis, such as using the output of 4D numerical weather models for computation of slant path delay in the neutral atmosphere, brightness temperature of the atmosphere, and atmospheric opacity. Leonid Petrov has managed project radio observations of unassociated *Fermi* sources and their follow-up with VLBI.

Management experience:

Managed twenty one projects under various astronomy programs at the National Radio Astronomical Observatory, Joint VLBI Institute in Europe, ATNF, the CSIRO's Australia Telescope National Facility, The Korean VLBI Network, and the National Astronomical Observatory of Japan.

Managed six ROSES projects under NASA programs as a principal investigator.

Education:

Ph.D. of Russian Academy of Sciences, 1995, Astronomy

M.S. of Leningrad National University, 1988, Astronomy

Selected publications: peer reviewed works

1. Giovannini, G., Savolainen, T., Orienti, M., Nakamura, M., Nagai, H., Kino, M., Giroletti, M., Hada, K., Bruni, G., Kovalev, Y. Y., Anderson, J. M., D’Ammando, F., Hodgson, J., Honma, M., Krichbaum, T. P., Lee, S.-S., Lico, R., Lisakov, M., M., Lobanov, A. P.; **Petrov, L.**, Sohn, B., W.; Sokolovsky, K. V.; Voitsik, P., A.; Zensus, J., A., Tingay, S., (2018). “A wide and collimated radio jet in 3C84 on the scale of a few hundred gravitational radii”, *Nature*, Doi: 10.1038/s41550-018-0431-2
2. **Petrov, L.**, Kovalev, Y.Y., (2017). “Observational consequences of optical range milliarcsecond-scale structure in active galactic nuclei discovered by Gaia”, *Mon. Not. Roy. Astr. Soc.*, 471, 3775–3787.
3. **Petrov, L.**, Kovalev, Y.Y., (2017). “On significance of VLBI/Gaia offsets”, *Mon. Not. Roy. Astr. Soc. Let.*, 467, L71–L75.
4. Kovalev, Y.Y., **Petrov, L.**, Plavin, A. V, (2017). “VLBI-Gaia offsets favour parsec-scale jet direction in Active Galactic Nuclei”, *Astron. & Astrophys.*, 598, L1.
5. Deller, A.T., Vigeland, S.J., D.L. Kaplan, W.M. Goss, W.F. Brisken, S. Chatterjee, J.M. Cordes, G.H. Janssen, T.J.W. Lazio, **L. Petrov**, B.W. Stappers, A. Lyne, (2016). “Microarcsecond VLBI pulsar astrometry with PSRPI I. Two binary millisecond pulsars with white dwarf companions”, *Astron J*, 828, 8D.
6. **L. Petrov**, E. K. Mahony, P. G. Edwards, E. M. Sadler, F. K. Schinzel, (2013). “ATCA observations of Fermi unassociated sources”, *Mon. Not. Roy. Astr. Soc.*, 432, 1294–1302.
7. **L. Petrov**, (2013). “The catalogue of positions of optically bright extragalactic radio sources OBRS-2”, *Astron J*, 146, 5
8. **L. Petrov**, G. Taylor, (2011). “Precise absolute astrometry from the VLBA imaging and polarimetry survey at 5 GHz”, *Astron J*, 142, 89.
9. **L. Petrov**, C. Phillips, A. Bertarini, T. Murphy, E. M. Sadler, (2011). “The LBA Calibrator Survey of southern compact extragalactic radio sources — LCS1”, *Mon. Not. Roy. Astr. Soc.*, 414(3), 2528–2539.
10. **L. Petrov**, Y. Y. Kovalev, E. B. Fomalont, D. Gordon, (2011). “The VLBA Galactic Plane Survey — VGaPS”, *Astron J*, 142, 35.
11. **L. Petrov**, Y. Kovalev, E. Fomalont, D. Gordon, (2008). “The sixth VLBA Calibrator Survey: VCS6”, *Astron J*, 136, 580.

There are 49 peer reviewed works with a total of 2171 citations. Hirsch index 19.

10 Summary of Work Effort

Table of Personnel and Work Effort

The following table reflects the level of support in FTE units required of all personnel (including unfunded co-investigators) necessary to perform the proposed investigation, regardless of whether these individuals require funding from this proposal.

Name	Role	Institution	PY 1	PY 2	Total
Leonid Petrov	PI	ADNET Systems	0.33	0.33	0.67
Alexander Plavin	collaborator	Astro Space Center	0.67	0.67	1.33
Yury Kovalev	collaborator	Astro Space Center	0.10	0.10	0.20

* — no budget is requested for foreign collaborates Alexander Plavin and Yury Kovalev. Alexander Plavin and Yury Kovalev. are funded at 1.0 FTE level from Lebedev Astro Space Center.

The proposed work level is appropriate to perform the investigation on the basis of previous investigations and experience.

PI Leonid Petrov will manage the project. He is responsible for retrieval of all space-born and ground-based observational data, cross-matching the sources from the parent sample with objects in the datasets under consideration and evaluation of the probability of false association. Leonid Petrov will compute the SED. He will be performing computation of dependencies of VLBI/*Gaia* offset parameters and evaluation of their significance. Leonid Petrov will develop SED models.

Collaborator Alexander Plavin, the 2nd year Ph.D. student, will investigate various relationships in VLBI/*Gaia* offset parameters with flux densities and spectral indices. He will be evaluating significance of these relationships. He will be reporting to prof. Yuri Kovalev.

Collaborator professor Yuri Kovalev will be involved in interpretation of relationships of VLBI/*Gaia* offset parameters and he will coordinate work of Alexander Plavin.

All team members will participate in writing the project report and a journal publication. Coordination of the project will be done mainly via email and telephone. The team will gather at the AAS and COSPAR meetings for face-to-face communication.